

**Pawel Witczak**  
**Technical University of Lodz**  
**Institute of Mechatronics and Information Systems**

## ANALYTICAL METHOD FOR CALCULATION OF EIGENFREQUENCIES AND MODES OF STATOR CORES IN AC MACHINES

**Abstract:** The paper describes analytical approach solving the problem of dynamic analysis of two-dimensional fields of vibrational displacements and rotations caused by forces acting on stator of AC machine. Final set of three differential equations converted into algebraic ones is given and it is confronted with numerical solutions obtained by finite element method.

### 1. Introduction

The question of magnetic vibration in AC machines becomes a quite frequent topic of investigations. The method commonly used is the finite element (FE) technique enabling the accurate analysis of free and forced vibration [2][9][10]. The geometry of the stator core together with its composite material structure is the reason of fact that FE mesh discretising the volume of stator core and windings contains the definite majority of all elements used in the overall model of the motor. That problem is particularly troublesome in the case of large machines, when the number of slots may exceed one hundred. Another difficulty arises, related to the solution time of the numerical model, when the vibration analysis should be directly incorporated into optimization routine. Even ten minutes or so necessary to solve the small FE model are too much if it is repeated few hundred times. Therefore, investigation of the fast and accurate method of vibration modeling seems still to be the important engineering subject in the domain of electric machines.

### 2. Mechanical model of smooth ring

#### 2.1. Plane displacements

Thick ring is the natural model of laminated stator core. Its dynamic behaviour under sinusoidal in space and time excitation is well known [1][7] – the equation describing its natural angular frequencies of  $n$ -th order is

$$\left(\frac{\omega_n}{\omega_0}\right)^2 = \beta \frac{n^2(n^2 - 1)^2}{(n^2 + 1)} \quad (1)$$

where  $\beta = h^2/12R^2$  -  $h$  is ring thickness and  $R$  denotes its mean radius, see fig.1. The normalisation constant  $\omega_0$  is so-called ring frequency (breathing mode) when ring surface moves

uniformly up and down in radial direction only. The value of this constant is given by

$$\omega_0^2 = \frac{E}{R^2 \rho} \quad (2)$$

where  $E$  is Young modulus and  $\rho$  is mass density. That model was starting point for the so-called “energy methods” [3][4].

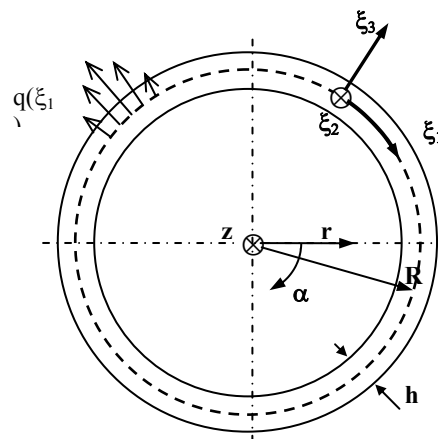


*Fig.1. Geometry of ring modeling stator lamination.*

Fundamental assumption of above model is sufficiently smaller ring thickness  $h$  than its mean radius  $R$ . Apart from global cylindrical system of coordinates  $r, \alpha, z$ , a local one  $\xi_1, \xi_2, \xi_3$  is also considered. Assuming that thickness  $h$  remains unchanged when the ring is deformed, one may introduce two functions of unknown magnitudes describing displacements of the mean ring surface (with  $r=R$ ) along angle  $\alpha$  in radial  $u_{30}$  and tangential  $u_{10}$  directions. If supporting system consists of virtual medium having very low stiffness and density these functions may be foreseen as

$$\begin{aligned} u_{10}(\alpha, t) &= U_1 \sin(n\alpha) e^{j\omega t} \\ u_{30}(\alpha, t) &= U_3 \cos(n\alpha) e^{j\omega t} \end{aligned} \quad (3)$$

Exciting forces of linear densities  $q_1(\alpha)$  and  $q_3(\alpha)$  have zero mean value along circumference. A classic, quite sophisticated analysis leads [1][7] to two differential equations

$$\begin{aligned} EI \frac{1}{R^4} \left( \frac{\partial^2 u_{10}}{\partial \alpha^2} - \frac{\partial^3 u_{30}}{\partial \alpha^3} \right) + E \frac{hg}{R^2} \left( \frac{\partial^2 u_{10}}{\partial \alpha^2} + \frac{\partial u_{30}}{\partial \alpha} \right) \\ = -q_1 + \rho gh \frac{\partial^2 u_{10}}{\partial t^2} \end{aligned} \quad (4)$$

$$\begin{aligned} EI \frac{1}{R^4} \left( \frac{\partial^3 u_{10}}{\partial \alpha^3} - \frac{\partial^4 u_{30}}{\partial \alpha^4} \right) - E \frac{hg}{R^2} \left( \frac{\partial u_{10}}{\partial \alpha} + u_{30} \right) \\ = -q_3 + \rho gh \frac{\partial^2 u_{30}}{\partial t^2} \end{aligned} \quad (5)$$

where  $I$  is the moment of inertia of the rectangular cross-section

$$I = \frac{gh^3}{12} \quad (6)$$

and  $g$  is the ring size along  $z$  axis. Introducing (3) into (4) and (5) one gets magnitudes  $U_1$ ,  $U_3$  and also, with  $q_1=q_3=0$ , the set of natural frequencies  $\omega_n$  shown earlier in eq. (1). Application of above equations to the problem of vibration of stator core is usually done by the simple increase of the ring density representing in that way the presence of stator teeth and windings. Unfortunately, such a treatment brings a considerable error, mostly for low values of  $n$ . Therefore, some modifications inside the model are necessary.

## 2.2 Plane displacements and rotation

Bending is dominating type of deformation of the ring geometry under forces of order  $n > 0$ . It means that radial component of displacement distribution along mean (neutral) surface has both positive and negative values. Simultaneously, the neutral surface remains stress free. It results that line  $Q_1 Q_2$  belonging to that surface and containing the point  $P_0$  of zero displacement preserves its length and is rotated only against this point, what is displayed in fig.2.

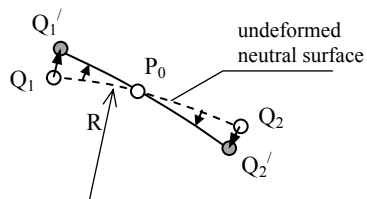


Fig.2. Explanation of rotation in bended ring.

The effect described is linked with the additional inertia related to the angular acceleration not included in previous model. It is possible to extend the set of unknown functions adding to eq. (3) the distribution of angular displacement  $\gamma$ .

$$\begin{aligned} \gamma(\alpha, t) &= \Gamma \sin(n\alpha) e^{j\omega t} \\ u_{10}(\alpha, t) &= U_1 \sin(n\alpha) e^{j\omega t} \\ u_{30}(\alpha, t) &= U_3 \cos(n\alpha) e^{j\omega t} \end{aligned} \quad (7)$$

Now three equations of motion are required for solution. They are obtained from infinitely small section of the ring being loaded by two-component force density applied to the neutral surface. The individual signs of force and torque components result from commonly used convention in mechanics [8]

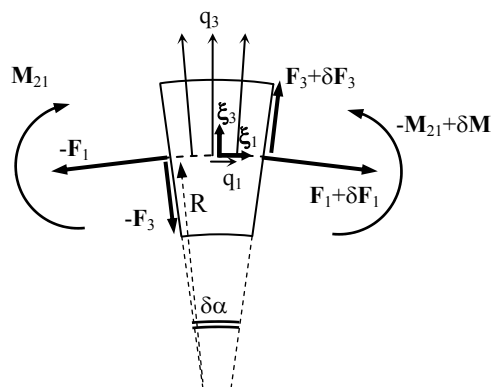


Fig.3. Geometry of ring section for equilibrium analysis.

The strain caused by the local rotation can be represented within theory of infinitesimal displacements by means of the shear strain  $\epsilon_{13}$ , which is given by

$$\epsilon_{13} = \frac{1}{2} \left( \frac{\partial u_{10}}{\partial \xi_3} - \frac{u_{10}}{R} + \frac{\partial u_{30}}{\partial \xi_1} \right) \quad (8)$$

where factor  $u_{10}/R$  includes reduction of radial shift by the tangent displacement due to ring curvature. Angle of rotation  $\gamma$  (between surfaces plotted in fig.2) may be represented by one of derivatives in (8) – they are in fact almost equal, but with opposite signs. Multiplying by shear stiffness  $2G$  and integrating over surface one gets the tangent force  $F_3$

$$F_3 = \kappa hgG \left( \gamma - \frac{u_{10}}{R} + \frac{\partial u_{30}}{R \partial \alpha} \right) \quad (9)$$

The coefficient  $\kappa$  equals to  $5/6$ , after Timoshenko theory [8].

The angular motion equation will be

$$+ \frac{\partial M_{21}}{\partial \alpha} - F_3 R = \rho I \frac{\partial^2 \gamma}{\partial t^2} R \quad (10)$$

The bending torque can be expressed [8] as

$$M_{21} = EI \frac{1}{R^2} \left( \frac{\partial u_{10}}{\partial \alpha} - \frac{\partial^2 u_{30}}{\partial \alpha^2} \right) \quad (11)$$

what finally gives

$$EI \frac{1}{R^2} \left( \frac{\partial^2 u_{10}}{R \partial \alpha^2} - \frac{\partial^3 u_{30}}{R \partial \alpha^3} \right) + \kappa h g G \left( \gamma - \frac{u_{10}}{R} + \frac{\partial u_{30}}{R \partial \alpha} \right) = \rho I \frac{\partial^2 \gamma}{\partial t^2} \quad (12)$$

We cannot use directly eq. (4)(5) as missing supplements for (12), because they were derived under assumption  $\varepsilon_{13}=0$  giving another than in eq. (9) expression for  $F_3$ . The equilibrium equations for movements along  $\xi_1$  and  $\xi_3$  have general form

$$\begin{aligned} \frac{F_3}{R} + \frac{\partial F_1}{R \partial \alpha} &= -q_1 + \rho g h \frac{\partial^2 u_1}{\partial t^2} \\ -\frac{F_1}{R} + \frac{\partial F_3}{R \partial \alpha} &= -q_3 + \rho g h \frac{\partial^2 u_3}{\partial t^2} \end{aligned} \quad (13)$$

Additions  $F_1/R$  and  $F_3/R$  arise from ring curvature. In order to get the relation describing  $F_1$  we have to know the membrane strain component along neutral layer – bending strain does not contribute to that force. Following strain definition we have

$$F_1 = E h g \left( \frac{1}{R} \frac{\partial u_{10}}{\partial \alpha} + \frac{u_{30}}{R} \right) \quad (14)$$

Substituting (9) and (14) into (13) we have

$$\begin{aligned} \frac{h g}{R} \kappa G \left( \gamma - \frac{u_{10}}{R} + \frac{\partial u_{30}}{R \partial \alpha} \right) + \\ \frac{h g}{R} E \left( \frac{1}{R} \frac{\partial^2 u_{10}}{\partial \alpha^2} + \frac{\partial u_{30}}{R \partial \alpha} \right) &= -q_1 + \rho g h \frac{\partial^2 u_1}{\partial t^2} \end{aligned} \quad (15)$$

$$\begin{aligned} \frac{h g}{R} \kappa G \left( \frac{\partial \gamma}{\partial \alpha} - \frac{\partial u_{10}}{R \partial \alpha} + \frac{\partial^2 u_{30}}{R \partial \alpha^2} \right) + \\ -\frac{h g}{R} E \left( \frac{\partial u_{10}}{R \partial \alpha} + \frac{u_{30}}{R} \right) &= -q_3 + \rho g h \frac{\partial^2 u_3}{\partial t^2} \end{aligned} \quad (16)$$

The next step it is to find magnitudes of investigated functions in eq. (7). Inserting these relationships into eq. (12)(15)(16), after few manipulations one may obtain the following set of equations, which is written in the classic form suitable both for forced and free vibration analysis

$$([\mathbf{A}] - \omega^2 [\mathbf{I}]) \begin{Bmatrix} \Gamma \\ U_3 \\ R \\ U_1 \\ R \end{Bmatrix} = \begin{Bmatrix} 0 \\ q_3 \\ \rho g h R \\ q_1 \\ \rho g h R \end{Bmatrix} \quad (17)$$

where  $[\mathbf{I}]$  is the identity matrix and  $[\mathbf{A}]$  matrix amounts to

$$[\mathbf{A}] = \begin{bmatrix} \omega_{GI}^2 & n(\omega_{GI}^2 - \omega_0^2 n^2) & \omega_0^2 n^2 - \omega_{GI}^2 \\ -n\omega_G^2 & \omega_G^2 n^2 + \omega_0^2 & n(\omega_G^2 + \omega_0^2) \\ -\omega_G^2 & n(\omega_G^2 + \omega_0^2) & \omega_G^2 + n^2 \omega_0^2 \end{bmatrix} \quad (18)$$

Particular constants denote

$$\begin{aligned} \omega_{GI}^2 &= \frac{\kappa g h}{\rho I} G \\ \omega_G^2 &= \frac{\kappa}{\rho h^2} G \\ \omega_0^2 &= \frac{1}{\rho R^2} E \end{aligned} \quad (19)$$

Further simplifications are possible dividing both sides of eq. (17) by  $\omega_0^2$ . For isotropic continuum modules  $E$  and  $G$  are directly proportional through  $2(1+\nu)$ . Setting Poisson coefficient  $\nu$  to 0.3 we have

$$\begin{aligned} \left( \frac{\omega_G}{\omega_0} \right)^2 &= \frac{\kappa}{2(1+\nu)} = i_G \cong 0.32 \\ \left( \frac{\omega_{GI}}{\omega_0} \right)^2 &= \frac{12\kappa}{2(1+\nu)} \left( \frac{R}{h} \right)^2 = i_{GI} \cong 3.84 \left( \frac{R}{h} \right)^2 \end{aligned} \quad (20)$$

Equations (17) are converted to

$$\left( [\mathbf{A}_0] - \left( \frac{\omega}{\omega_0} \right)^2 [\mathbf{I}] \right) \begin{Bmatrix} \Gamma \\ U_3 \\ R \\ U_1 \\ R \end{Bmatrix} = \frac{1}{\omega_0^2} \begin{Bmatrix} 0 \\ q_3 \\ \rho g h R \\ q_1 \\ \rho g h R \end{Bmatrix} \quad (21)$$

and matrix  $[\mathbf{A}_0]$  amounts to

$$[\mathbf{A}_0] = \begin{bmatrix} i_{GI} & n(n^2 - i_{GI}) & n^2 - i_{GI} \\ -ni_G & n^2 i_G + 1 & n(i_G + 1) \\ -i_G & n(i_G + 1) & i_G + n^2 \end{bmatrix} \quad (22)$$

Coefficients of  $[\mathbf{A}_0]$  depend on dimensionless values of the mode order  $n$  and the ratio  $(R/h)^2$  only. Comparing results obtained by the above approach with previously described method using displacements only, we will get very similar results, therefore, introduction of rotation is not mandatory while the smooth ring is analysed. On other hand, the presence of rotation in description of ring motion enables the further development of this model towards the proper representation of slotted structure.

### 3. Mechanical model of stator lamination

Geometry of lamination sheet of typical multi-pole AC motor – in example given below  $2p=8$ , is presented in fig.3. It is assumed that no constraints exist in surrounding medium and also external forces of electromagnetic nature belong to  $\mathbf{r}\alpha$  plane and they are balanced in space and time.

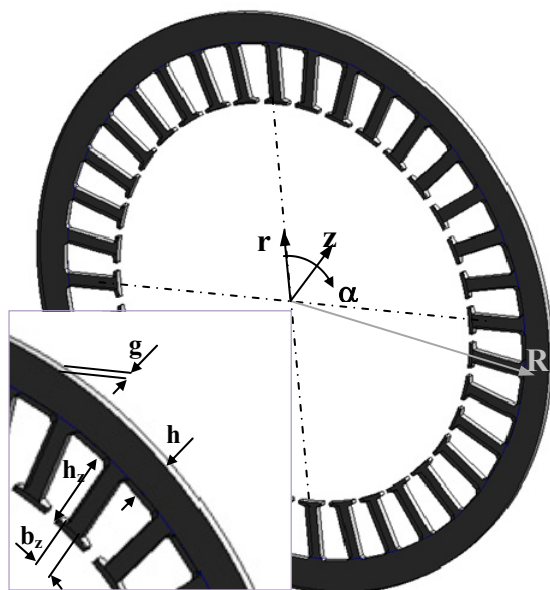


Fig.4. Geometry of single lamination sheet of AC motor.

The key assumption in modeling the behaviour of stator teeth is that they follow the local yoke displacements and rotation in form of the rigid body motion. It means that presence of teeth on one side of the ring changes its inertial properties only. The inertial term in equations (15)(16) is related to displacements, therefore, mass density must be increased by the ratio  $k_\rho$  of lamination to yoke mass,

$$k_\rho = 1 + \frac{Qb_z h_z}{2\pi R h} \quad (23)$$

where  $Q$  is number of teeth and remaining dimensions are displayed in fig.4. The modification of eq. (12) is a bit more complicated. We want to account the increase of angular inertia of continuous ring structure, which was induced by the discrete set of teeth. It will be done in few steps. Firstly, the real shape of single tooth is reduced to the rectangle as it is shown in fig.5.

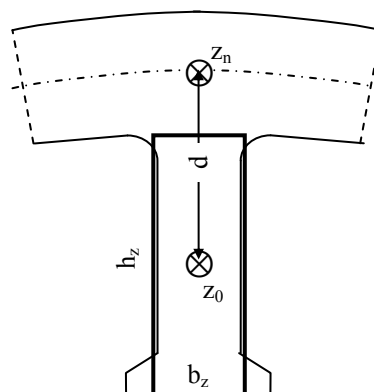


Fig.5. Simplified geometry of lamination tooth.

The main moment of inertia of the cuboid against axis passing through its gravity center is

$$J_{z_0} = \rho I_{z_0} \left( 1 + \left( \frac{b_z}{h_z} \right)^2 \right) b_z \quad (24)$$

where  $I_{z_0}$  is moment of inertia of the rectangle ( $h_z, g$ ) against its symmetry axis along side  $g$ . Tooth is rotated about axis  $z_n$  situated on neutral layer, so, after Steiner theorem, the moment of tooth inertia about  $z_n$  equals to

$$J_{z_n} = J_{z_0} + m_z d^2 \quad (25)$$

where  $m_z$  is the tooth mass. After few manipulations we may have

$$J_{z_n} = \rho I_{z_0} \left[ 1 + \left( \frac{b_z}{h_z} \right)^2 + 3 \left( 1 + \frac{h}{h_z} \right)^2 \right] b_z \quad (26)$$

The ring equation (12) requires continuous properties like linear force density, therefore, we must “spread” inertia  $J_{z_n}$  along slot pitch measured on neutral layer. It may be now added to the moment of inertia of the yoke cross-section (6). It will be done by means of multiplication factor  $k_I$  increasing the value of  $I$ .

$$k_I = 1 + \left( \frac{h_z}{h} \right)^3 \left[ 1 + \left( \frac{b_z}{h_z} \right)^2 + 3 \left( 1 + \frac{h}{h_z} \right)^2 \right] \frac{Qb_z}{2\pi R} \quad (27)$$

The change of the overall mass also influences the value of reference angular frequency  $\omega_0$

$$\omega_{0z}^2 = \frac{\omega_0^2}{k_\rho} \quad (28)$$

Finally, substituting all additions (23)(27)(28) related to the presence of slots it is possible to write the set of equations (21) in form

$$\left( [\mathbf{A}_{0z}] - \left( \frac{\omega}{\omega_{0z}} \right)^2 [\mathbf{I}] \right) \begin{Bmatrix} \Gamma \\ \frac{U_3}{R} \\ \frac{U_1}{R} \end{Bmatrix} = \frac{k_p}{\omega_0^2} \begin{Bmatrix} 0 \\ q_3 \\ \rho ghR \\ q_1 \\ \rho ghR \end{Bmatrix} \quad (29)$$

and corrected matrix  $[\mathbf{A}_{0z}]$  is given by

$$[\mathbf{A}_{0z}] = \begin{bmatrix} \frac{k_p}{k_l} i_{G1} & n \frac{k_p}{k_l} (n^2 - i_{G1}) & \frac{k_p}{k_l} (n^2 - i_{G1}) \\ -ni_G & n^2 i_G + 1 & n(i_G + 1) \\ -i_G & n(i_G + 1) & i_G + n^2 \end{bmatrix} \quad (30)$$

Solving the eigenvalue problem for exemplary lamination in two ways – analytical, based on equations (29)(30) and numerical by FE approach, the results obtained are confronted in table 1.

Table 1. Comparison of analytic and numeric solutions of relative natural frequencies obtained for sheet given by:  $Q=36$ ,  $R=0.08$  m,  $h=0.01$  m,  $h_z=0.018$  m,  $b_z=0.004$  m,  $k_p=1.49$ ,  $k_l=14.2$ .

Method	relative natural frequency $\omega_n/\omega_{0z}$			
	$n=2$	$n=3$	$n=4$	$n=5$
analytic	0.091	0.252	0.467	0.728
numeric	0.091	0.245	0.441	0.642

Ring frequencies were – for analytic calculations  $\omega_{0z}=49.21 \cdot 10^3$  rad/s] and for numeric ones  $\omega_{0z}=48.62 \cdot 10^3$  [rad/s]. The agreement obtained for the lowest modes is very good, for higher modes a few percent discrepancy has appeared. It can be explained observing the shapes of investigated modes visualised by FE software in fig.6. Looking on the lowest mode of order  $n=2$  we see that all teeth are perpendicular to deflected mean line of yoke fulfilling in that way the assumption of purely inertial nature of vibrational behaviour of teeth. But in the case of higher order  $n=5$  one can see the bended outline of the most of teeth. It means stator teeth do not behave like rigid body as it was assumed initially. That influence on values of calculated natural frequencies is not very substantial but visible. This effect is a natural limit of presented method.

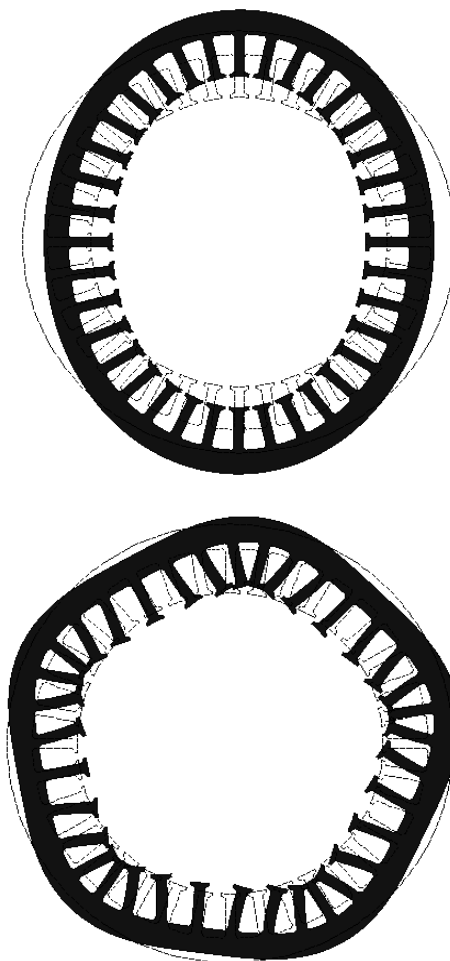


Fig.6. Shapes of natural modes of order  $n=2$  and  $n=5$ .

#### 4. Conclusions

The calculation method described in the paper enables the fast and accurate estimation of natural frequencies for modes of the lowest order. It means that it can be also applied for forced vibration in a quite wide range of exciting frequencies. Its accuracy near resonances will not be very good because of the absence of components representing the energy dissipation in equations of motion. They may be added in a standard way [5][6] converting solution into complex domain. The another application foreseen in a future work is the search of equivalent anisotropic ring structure for slotted lamination. Such a problem cannot be solved explicitly because of its nonlinear relationships – it requires iterative approach, where a computation time is one of decisive factors when the method of modeling is chosen.

## 5. Bibliography

- [1] L.Cremer, M.Heckl, B.A.T.Petersson, *Structure – Borne Sound*, Springer Verlag, Berlin 2005
- [2] Delaere K. *Computational and experimental analysis of electric machine vibrations caused by magnetic forces and magnetostriction*, PhD Thesis, Katholieke Universiteit Leuven, 2003
- [3] Ellison A J and S J Yang. *Natural Frequencies of Stators of Small Electric Machines*. Proceedings of the IEE, 118(1):185–190, 1971
- [4] Girgis R.S. and Verma S.P. *Method for Accurate Determination of Resonant Frequencies and Vibration Behaviour of Stators of Electrical Machines*. Electric Power Applications, IEE Proceedings B, 128(1):1–11, 1981
- [5] Norton M., Karczub D., *Fundamental of Noise and Vibration Analysis for Engineers*, Cambridge University Press, 2003
- [6] Rao S.S., *Vibration of continuous systems*, John Wiley & Sons Inc., 2007
- [7] Soedel W., *Vibration of shells and plates*, Marcel Dekker Inc., 2004
- [8] Timoszenko S., Goodier J.N., *Teoria sprężystości*, Arkady, Warszawa, 1962
- [9] Wang H. and Williams K. *The Vibrational Analysis and Experimental Verification of a Plane Electrical Machine Stator Model*. Mechanical Systems and Signal Processing, 9(4):429–438, 1995
- [10] Witczak P., *Wyznaczanie drgań mechanicznych w silnikach indukcyjnych wywołanych siłami magnetycznymi*, Zesz. Nauk. Politechniki Łódzkiej nr 725, 1995, Łódź

### Author

Pawel Witczak, PhD, DSc, Technical University of Lodz, Institute of Mechatronics and Information Systems, Stefanowskiego 18/22, 90-924 Lodz, Poland, phone/fax (+48)42 631 2580/ (+48)42 636 2309 pwitczak@p.lodz.pl,

### Reviewer

Prof. dr hab. inż. Krzysztof Kluszczyński